Synthesis and Biological Evaluation of New Citrate-Based Siderophores as Potential Probes for the Mechanism of Iron Uptake in Mycobacteria

Hongyan Guo,[†] Saleh A. Naser,[‡] George Ghobrial,[‡] and Otto Phanstiel IV*,[†]

Center for Discovery of Drugs and Diagnostics, Department of Chemistry, and Department of Molecular and Microbiology, University of Central Florida, Orlando, Florida 32816-2366

Several iron chelators containing α,β-unsaturated hydroxamic acid motifs appended to a citric acid platform were synthesized. *Mycobacterium paratuberculosis* was then challenged to grow in the presence of a panel of siderophores (mycobactin J, deferrioxamine B, acinetoferrin, and nannochelin A) and the new synthetic agents. Of the structures tested, those containing the trans 2-octenoyl motif were preferred over those with trans cinnamoyl groups. In addition, derivatives containing longer tether lengths between the iron binding ligands (C5) were more efficacious and led to higher growth index values. Perhaps most remarkable was the finding that at 2.4 μM a trans 2-octenoylated, citrate-containing imide **6** was nearly 5-fold more effective in stimulating growth than the native chelator, mycobactin J. In this regard, new structural elements were identified (e.g., an imide motif or 2-octenoyl side chain), whose presence stimulated mycobacterial growth.

Introduction

The World Health Organization (WHO) estimates that there were 8.4 million new cases of tuberculosis (TB) in 1999 and that the annual global rate of increase in TB incidence was 3%.[1] Assuming this rate of increase persists, there will be over 10 million new cases of TB in 2005.[1] Moreover, *Mycobacterium tuberculosis*, the organism that causes the disease, has proven to be very resilient. The recent emergence of multidrug resistant (MDR) strains is of special concern due to the reported high death rates associated with MDR TB.[2,3] In addition, the current treatment of MDR strains is 100 times more expensive than with drug-susceptible strains.[2] In short, tuberculosis continues to be a public health threat, to the extent that the WHO has declared tuberculosis as a global public health emergency.[1]

Infection of a host by *M. tuberculosis* results from the inhalation of droplet nuclei containing the organism. Colonization of the organism takes place in the alveolar sacs in the lungs, where it encounters macrophages of the immune system. Macrophages that are attracted to the area by phagocytic cells, T-cells, and other immune cells fuse to form giant cells in the vicinity of the damaged tissue containing the bacteria.[4] These macrophages as well as other immune cells wall-off the growing culture with a thick fibrin coat.[4] This is the tubercle or lesion that is associated with the disease. Like most mycobacteria, cells of *M. tuberculosis* are covered by a lipid-rich cell wall comprised mainly of a large amount of mycolic acids containing long hydrocarbon chains (Figure 1). The length and high degree of saturation of the chains produce an exceptionally tightly packed array with extremely low fluidity.[5]
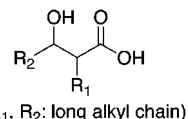

Figure 1. Mycolic acid architecture.

(R₁, R₂: long alkyl chain)

Consequently, penetration of antibiotics and chemotherapeutic agents through both the resulting tubercle and bacterial cell wall is limited.[5,6] The design and synthesis of an efficient drug carrier, which facilitates drug delivery, has become a major challenge in anti-TB drug development.[7,8] Therefore, understanding mycobacterial transport processes may offer new strategies to combat this microorganism.

Virulence and even survival of most microbes during infections depend on their ability to compete effectively for key nutrients such as iron. However, iron exists mainly as insoluble ferric hydroxide polymers in the biosphere and is sequestered in humans by high molecular weight proteins such as transferrin (Fe transport) and ferritin (Fe storage). Microorganisms have evolved ferric ion (Fe^{3+}) specific chelating agents, i.e., siderophores,[9] which can solubilize and transport iron to the microbe. These low molecular weight ligands have been shown to rapidly remove iron from human proteins such as transferrin.[10] Then, by modification, reduction, or siderophore decomposition, iron is released for use by the cell.[10] Most mycobacteria produce two types of siderophores: exochelins, which are secreted extracellularly, and mycobactin, which is cell wall associated.[11a] As shown in Figure 2 [mycobactin J **1**, deferrioxamine B (DFO, shown as its mesylate salt) **2** from *Streptomyces pilosus*, nannochelin A **3** from *Nannocystis exedens*, a hydrophilic exochelin found in *M. tuberculosis* cultures (carboxymycobactin) **4**,[10] acinetoferrin **5** from *Acinetobacter haemolyticus*, and acinetoferrin imide **6**], the overall structures of siderophores vary depending upon their microbial source. The iron-binding functional groups incorporated into siderophores by most microbes

---

* To whom correspndence should be addressed. Tel.: 407-823-5410. Fax: 407-823-2252. E-mail: ophansti@mail.ucf.edu.
    † Center for Discovery of Drugs and Diagnostics, Department of Chemistry, University of Central Florida.
    ‡ Department of Molecular and Microbiology, University of Central Florida.
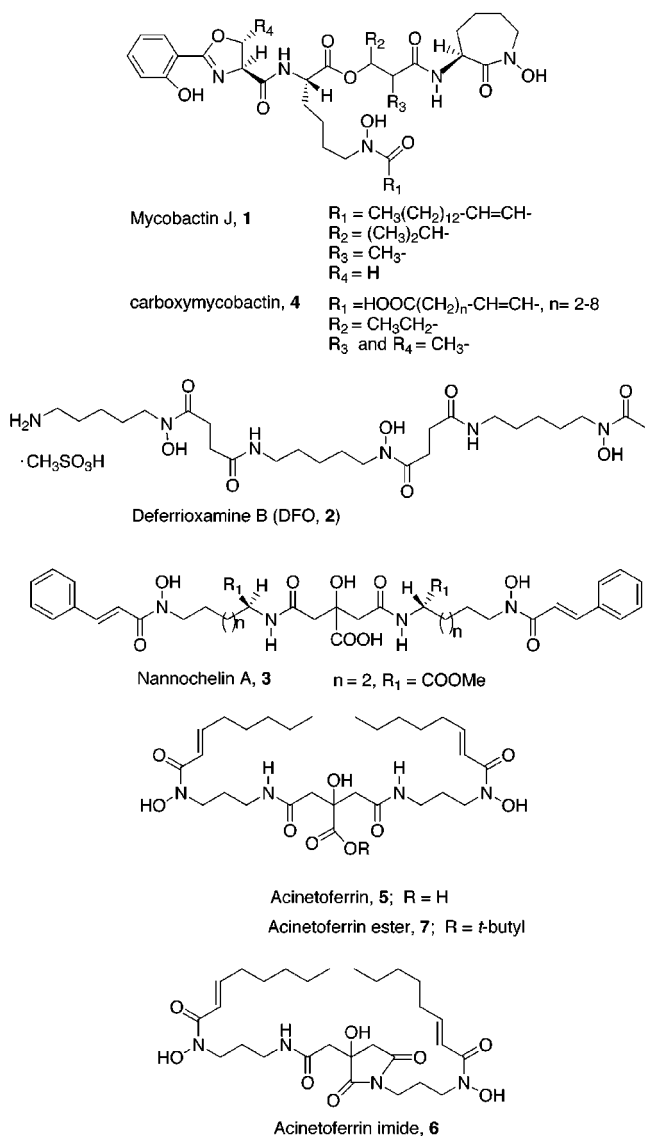
Figure 2. Structures of iron chelators.

have been conserved and are limited primarily to hydroxamic acids, catechols, and α-hydroxy-carboxylic acids.[9] By design, the hexadentate architectures containing these oxygen-rich, bidentate subunits have a high affinity for binding ferric ion.[9]

Because iron is essential for the growth and survival of *M. tuberculosis*, several approaches have been suggested for the development of antibiotics based on siderophores and their analogues.[7,8,10] One approach is the development of conjugates (containing a lethal drug covalently attached to a siderophore), which may lead to new forms of drug delivery that utilize the pathogenic organism's own iron transport system. In this regard, the siderophore represents a "tunable" vector for the delivery of organism specific antibiotics.[10] Another approach is to sequester the available iron into a form, which cannot be processed by the bacteria. The success of this latter approach relies on understanding the molecular recognition events involved in mycobacterial iron transport.

Targeting the iron transport processes of *M. tuberculosis* is challenging for several reasons. First, the complexity of the mycobactin architecture itself poses a daunting synthetic challenge, which hampers the generation of conjugates.[5b] Second, the iron transport mechanism involves an "iron-handoff" between two siderophore families, the exochelins and the mycobactins. In low iron environments, *M. tuberculosis* biosynthesizes and secretes hydrophilic exochelins (e.g., **4**) to bind exogenous ferric ion. The iron-laden complex is then transferred to intracellular siderophores, i.e., the mycobactins, which are lipophilic chelators associated with the cytoplasmic membrane.[10] The mycobactin-associated iron either remains in the cell wall as an iron storage pool or is released into the cell by a mycobactin reductase.[10]

This paper describes the synthesis and biological evaluation of several new citrate-based siderophores as potential probes to study the iron uptake mechanisms of mycobacteria.[12] A panel of siderophores with low, moderate, and high growth stimulation effects would be useful in comparing the iron uptake processes of genetically modified mycobacterial strains with their native counterparts. The focus of this investigation was to develop a structure–activity relationship between citrate-based iron chelators and their effect on the growth rate of *Mycobacterium paratuberculosis. M. paratuberculosis* was chosen as an alternative pathogenic model for *M. tuberculosis* and is responsible for Johne's disease (an inflammatory bowel disease in cattle) and Crohn's disease in humans.[11] Because *M. paratuberculosis* relies upon the addition of exogenous mycobactin J (Figure 2) to grow in vitro, it serves as a sensitive model for iron acquisition studies.[13] Beyond direct insight into possible new Crohn's disease probes, the findings gained with this organism should also apply to its virulent cousin, *M. tuberculosis.* The expectation was that iron-binding ligands, which were readily utilized by *M. paratuberculosis*, could eventually serve as mechanistic probes for both *M. paratuberculosis* and *M. tuberculosis.*

Previously, two citrate derivatives were synthesized in our laboratory, acinetoferrin **5** (from *A. haemolyticus* ATCC 17906) and acinetoferrin imide **6** (Figure 2).[14] Preliminary screens indicated that imide **6** was superior to mycobactin J in "cross-feeding" *M. paratuberculosis.* Armed with this insight, we synthesized a series of citrate derivatives to identify which structural features of **6** were responsible for its remarkable activity.

Results and Discussion

As shown in Figure 2, mycobactin J[13] and DFO (the native chelator for *Streptomyces pilosus*)[15] are predicated upon α-amino acid and polyamide backbones, respectively. The hydroxamic acid (RCON(OH)R′) and the α-hydroxy carboxylic acid components are responsible for iron chelation.[9,16] Thus, each siderophore represents a hexacoordinate ligand for iron(III). Both acinetoferrin **5** and its imide **6** contain the unusual trans-2-octenoyl hydroxamic acids appended to a citric acid framework. Indeed, the ability of acinetoferrin imide **6** to cross-feed mycobacterial strains may stem from its appended long hydrophobic alkyl tail.[5b,17] To probe this insight, we used a modular synthetic approach,[14,16,18] which allowed for alteration of the terminal hydrophobic "tails" and the aliphatic spacer separating the bidentate ligands.

Synthesis. For comparison purposes, acinetoferrin,[14] acinetoferrin *tert*-butyl ester **7**,[14] and nannochelin A **3**[18]
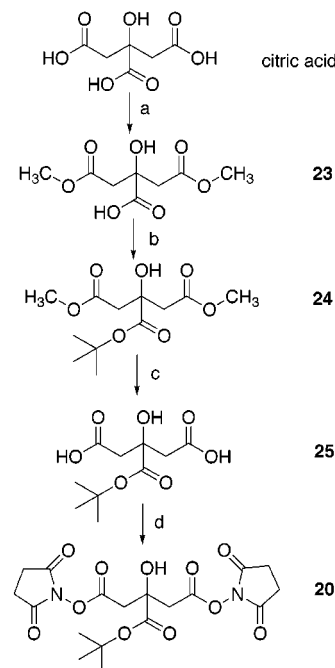
Scheme 1[a]
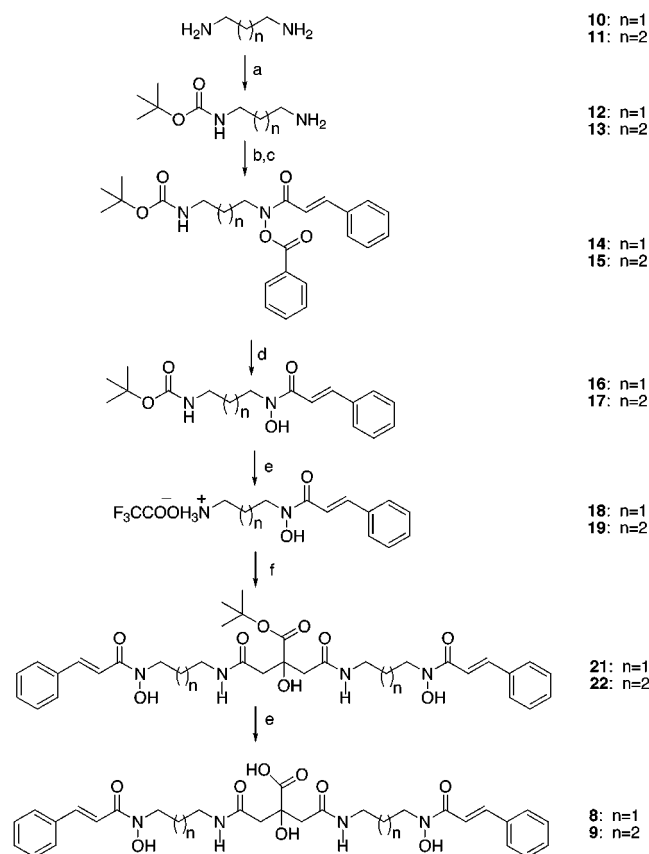
[a] Reagents: (a) Di-*tert*-butyl dicarbonate, 10% TEA/MeOH; (b) benzoyl peroxide (2 equiv)/CH_2Cl_2, pH = 10.5 aqueous sodium carbonate buffer, room temperature; (c) *trans*-cinnamoyl chloride, CH_2Cl_2; (d) 10% NH_4OH/MeOH; (e) TFA, 0 °C; (f) TEA, **20**, dry dioxane, 0 °C.

Scheme 2[a]

[a] Reagents: (a) Concentrated H_2SO_4, MeOH; (b) concentrated perchloric acid, *tert*-butyl acetate, room temperature, 3 days; (c) 2 M aqueous NaOH in MeOH, 3 h; (d) *N*-hydroxysuccinimide, DIC, dry THF.

were also acquired by published procedures. To test the side chain premise, new derivatives with appended trans cinnamoyl groups were envisioned. The trans cinnamoyl group represented another hydrophobic group (in lieu of the trans 2-octenoyl tail) with the same carbon count but with reduced conformational freedom. As shown in Scheme 1, two carbon tethers ($n = 1$ and 2) were incorporated into the new derivatives **8** and **9**, respectively.

The synthesis of the new derivatives involved a series of protection and deprotection steps similar to those outlined in our total synthesis of acinetoferrin.[14] In 1990, Milewska et al. illustrated the formation of an *O*-benzoyl-protected hydroxamate using benzoyl peroxide (BPO) followed by acetyl chloride.[19] This approach led to an improved amine-oxidation method involving biphasic conditions, which was used successfully in this and other reports.[14,20–22] The strategy involved the construction of a *N*-(alkylamino)-*N*-hydroxyl-*trans*-cinnamamide precursor via a tandem oxidation-acylation of the primary amino group of a protected diamine derivative. This elaboration was completed prior to coupling with the terminal carboxylic acid groups of a citric acid derivative. Previous experience revealed that higher yields were obtained in the condensation step, if the benzoyl group was removed prior to amide formation.[14,18]

As shown in Scheme 1, the reaction of either diamine (**10** and **11**) with di-*tert*-butyl dicarbonate afforded the

mono BOC-protected amines (**12** and **13**) in 82 and 75% yield, respectively. Compounds **12** and **13** were each dissolved in a biphasic mixture containing carbonate buffer, pH 10.5, and BPO dissolved in CH_2Cl_2. After the oxidation step, each mixture was then acylated with *trans*-cinnamoyl chloride to give the desired compound **14** (55%) and **15** (52%), respectively. These represent significant increases in yield as compared to earlier efforts with nannochelin A, **3** (25% yield).[18] Compounds **14** and **15** were then treated with a 10% concentrated NH_4OH in MeOH solution at 0 °C to liberate the "free" hydroxamic acid **16** (81%) and **17** (94%), respectively. Treatment of **16** and **17** with trifluoroacetic acid (TFA) at 0 °C removed the BOC group and produced the respective TFA salts **18** and **19**. As shown in Scheme 1, condensation of **18** and **19** with **20** in 1,4-dioxane gave **21** (90%) and **22** (85%), respectively. Finally, treatment of **21** and **22** with TFA gave the respective chelators **8** (89%) and **9** (84%).

While the selective coupling of amino substrates with the terminal carboxyls of citric acid can be achieved utilizing either 2-substituted-1,3-bis-activated esters of citric acid or anhydromethylene citric acid,[16,23] the reported imide formation associated with the latter approach prompted the use of the former coupling methodology. The selective activation of the 1,3-carboxyls of citric acid was accomplished via the terminally bis-activated ester 2-*tert*-butyl-1,3-di-*N*-hydroxy-succinimidyl citrate (bis-NHS ester, **20**).

As shown in Scheme 2, **20** was prepared using a modification of Milewska's original method utilizing intermediates **23**–**25**.[16] *N*,*N*-Diisopropylcarbodiimide was used as the condensation reagent instead of *N*,*N*-dicyclohexylcarbodiimide in the last step to facilitate isolation of the diamide.[12,24]

Table 1. GI for *M. Paratuberculosis* in the Presence of Iron-Binding Ligands at 2.4 μM[a,b]

no. (compd)	reading	GI[a]
1 (mycobactin J)	601	1
2 (DFO)	552	0.92
5 (acinetoferrin)	607	1
7 (acinetoferrin *tert*-butyl ester)	412	0.69
8 (C3 cinnamoyl)	458	0.76
9 (C4 cinnamoyl)	924	1.5
21 (C3 cinnamoyl *tert*-butyl ester)	539	0.90

[a] GI values were normalized to Mycobactin J growth activity. [b] The sterile broth media contained ferric ammonium citrate (0.04 g/L media).

Table 2. GI for *M. Paratuberculosis* in the Presence of Iron-Binding Ligands at 2.4 μM[a,b]

no. (compd)	reading	GI[a]
1 (mycobactin J)	152	1
2 (DFO)	146	0.96
3 (nannochelin A)	379	2.5
6 (acinetoferrin imide)	703	4.6

[a] GI values were normalized to Mycobactin J growth activity. [b] The sterile broth media contained ferric ammonium citrate (0.04 g/L media).

Biological Evaluation. All derivatives tested were capable of forming hexadentate-binding architectures. Note: the *tert*-butyl ester in **21** could form an overall hexadentate ligand via its two hydroxamic acid motifs and the available α-hydroxycarbonyl bidentate site. The respective siderophores and synthetic derivatives (**1**–**3**, **5**–**9**, and **21**) were evaluated for their ability to act as growth factors for *M. paratuberculosis* at 2.4 μM (a standard concentration used routinely with **1** in *M. paratuberculosis* cultures).[13,25] Several controls were run in tandem. Mycobactin J (the native chelator, **1**) provided the benchmark control. In this manner, systems that provided significantly higher growth index (GI) values than the native chelator **1** (GI = 1) were identified as superior growth stimulants and more efficacious iron delivery agents (vide infra). In addition, DFO **2** probed the effect of simply providing solubilized ferric ion as the determining factor in stimulating growth. If no molecular recognition events were involved, all of the ligands tested would have provided approximately the same growth index. As shown in Tables 1 and 2, this was clearly not the case.

One can compare the tabular data (Tables 1 and 2) as all siderophores were dosed at the same concentration (2.4 μM) in the same media with the same cell type and uniformly cultured under the same environmental conditions (see Experimental Section). Although the biological evaluations listed in Table 2 were performed separately, they were performed in the presence of the appropriate controls for proper comparison. The diverse growth rates observed with these systems required that measurements of "fast" growing cultures (e.g., with **6**) be conducted separately as they generated the maximum reading (999) from the BACTEC instrument at earlier times (see Experimental Section).

As shown in Table 1, mycobactin J **1**, DFO **2**, acinetoferrin **5**, and C3 ester **21** gave comparable results, while acinetoferrin ester **7** and C3-cinnamoyl derivative **8** had marginally lower activity. Interestingly, the C4 cinnamoyl analogue **9** had a higher GI than **1**. In general, the systems containing longer tethers gave higher GI values (e.g., GI for C3 **8**, 0.76, vs C4 **9**, 1.5). Table 2 further illustrates the influence of tether and other structural features on the GI value. The tether trend is likely reflected in Table 2 with nannochelin A **3**, which contains a C5 tether and a relative GI of 2.5. We speculate that the longer tether allows for a more conformationally flexible ligand to properly coordinate to iron and provides an incremental increase in hydrophobicity. Such tether effects have been observed with other siderophore systems such as DFO **2**. In fact, molecular modeling studies with DFO suggest that tethers, which are too short (<C5), may compromise the optimum binding geometry around iron by perturbing the octahedral complex.[9b]

A priori, one may have expected that the more hydrophobic esters would be uniformly more efficacious than their carboxylic acid counterparts. This was not the case in the limited number of systems examined. Replacement of the free carboxylic acids in **5** and **8** with *tert*-butyl esters (**7** and **21**, respectively) gave similar values and no clear trend. In hindsight, this result is not surprising as the ester does not preclude the hexadenticity of **7** and **21** and other structural factors may dominate such as tether length. The observation that bulky *tert*-butyl esters did not dramatically alter growth provides a possible site for future modifications of the acyclic scaffold.

Comparison of the trans 2-octenoyl side chain present in **5** with the trans cinnamoyl analogue present in **8** reveals a preference for the octenoyl subunit (GI for **5**, 1.0, vs **8**, 0.76). We speculate that the conformational freedom of the octenoyl side chain may enable more favorable membrane interactions with a cell–surface receptor or via simple chain entanglements. Interestingly, the 2-octenoyl subunit may play other roles in mycobacteria. First, it resembles a precursor to the mycolic acid constituents of the mycobacterial cell wall (Figure 1) and the R_1 side chain of mycobactin J (Figure 2). Second, in studies of isoniazid and ethionamide resistant *M. tuberculosis* strains, a single missense mutation in the *inhA* gene confers resistance to both drugs. Recently, the corresponding InhA protein was shown to be a NADH specific enoyl reductase, involved in the synthesis of fatty acids in mycobacteria.[26] Interestingly, 2-trans-octenoyl ACP and 2-octenoyl-CoA were also substrates for the InhA protein.[26]

Perhaps the most exciting finding from this study was the nearly 5-fold growth increase of *M. paratuberculosis* in the presence of acinetoferrin imide **6** (GI = 4.6) vs the control platform (mycobactin J, GI = 1, Table 2). Compound **6** represented another structural refinement (e.g., imide formation) that influenced ligand efficacy (i.e., GI value). Comparison of acyclic **5** (C3 tether, GI = 1) and imide **6** (C3 tether, GI = 4.6) revealed the significance of the cyclic architecture. The fact that both native chelators (**1** and **4**) as well as **6** each contain a cyclic bidentate ligand within their architectures may be more than a curious coincidence and deserves further study.

The trends identified in this investigation point to future alterations in the chelator architecture, which should result in an even more efficacious ligand. In this manner, future ligands could be optimized by including the most preferred structural elements of the series studied. Although **6** contained the preferred octenoyl

subunits, it also contains the shortest tether (C3). A logical extension of these studies is to change the carbon tether to a five methylene bridge (C5), while maintaining the imide framework. Ironically, the anhydromethylene synthetic pathway[16,23] we originally sought to avoid[14] may, in hindsight, offer access to these novel imide platforms. Although the imide blocks attachment to the central citrate core via an ester linkage (e.g., **7**) and thereby limits other possible structural modifications, its efficacy warrants future investigation.

Conclusions

An efficient, modular approach to the construction of α,β-unsaturated hydroxamic acids[14] was applied to the construction of several citrate derivatives. The biological studies suggest that the iron-uptake events in *M. paratuberculosis* involve molecular recognition events, which (i) prefer trans 2-octenoyl groups over cinnamoyl side chains (e.g., **5** vs **8**) and (ii) favor an imide motif over an acyclic architecture (e.g., **6** vs **5**). In summary, the structure–activity relationships developed in this paper have identified new synthetically accessible ligands, which are structurally less complex than mycobactin J and have different affinities for the iron-uptake apparatus of mycobacteria. Such ligands, which offer regulation of the initial iron delivery step, provide the opportunity to compare the iron transport mechanisms of both native and genetically modified mycobacteria.[25]

Experimental Section

Materials and Methods. Lipophilic Sephadex LH-20 was obtained from the Sigma Chemical Company. Silica gel (32–63 μm) was purchased from Scientific Adsorbents, Inc. *Trans*-2-octenoic acid (97.1% pure) was purchased from Lancaster Synthesis, Inc. Reagents were purchased from the ACROS Chemical Company and used without further purification. All solutions are expressed in volume percent. Ammonia-containing solutions were prepared by measuring out concentrated aqueous NH_4OH in the listed volume percent. The pH 10.5 carbonate buffer solution was prepared by combining 222 mL of 0.75 N aqueous $NaHCO_3$ and 78 mL of 1.5 N aqueous NaOH. "Iron-free" glassware was obtained by soaking the glassware in a 6 N HCl bath overnight and then washing with deionized water. Deionized water was obtained from a "B-pure" filtration system by collecting the water when the "in-line" electrical resistance was 17.0 MΩ cm. Iron-free silica gel was made by washing with methanol:acetone:10 M HCl (45:45:10), followed by 10% (w/w) Na_2CO_3 solution and then rinsed with deionized water until pH 7 and air-dried. ^1H and ^{13}C nuclear magnetic resonance (NMR) spectra were recorded at 200 MHz on a Varian XL-200 spectrometer. The mass spectra were performed at the University of Florida Department of Chemistry by Dr. David Powell. Mycobactin J **1** and DFO **2** were purchased from Allied Monitor Company in Fayette, MO, and the Sigma-Aldrich Chemical Co., respectively. Nannochelin A **3**,[18] acinetoferrin **5**,[14] acinetoferrin imide **6**,[14] and acinetoferrin *tert*-butyl ester **7**[14] were acquired from published methods. Beyond the "clean" NMR spectra obtained for both **8** and **9**, their purities were assessed by eluting each substance in two different thin-layer chromatography (TLC) systems, which confirmed the homogeneity of the sample. The procedures used to make **20** and **23**–**25** are also included to illustrate the changes made to Milewska's procedures.[16]

Bioassay. BACTEC 12B Mycobacteria also known as Middlebrook 7H12 Medium was purchased from Becton Dickinson (Pittsburgh, PA). It contains 7H9 broth base, casein hydrolysate, bovine serum albumin, catalase, and palmitic acid labeled with ^{14}C. It is specific for growing mycobacteria and is used in conjunction with the BACTEC brand 460 TB Analyzer. The Middlebrook 7H9 broth base media consists of 4 mL of broth mixture included in a sealed bottle. The bottles, therefore, contain 7H9 and other ingredients such as ammonium sulfate, glutamic acid, sodium citrate, pyridoxine, biotin, disodium phosphate, ferric ammonium citrate (0.04 g/L media), magnesium sulfate, calcium chloride, zinc sulfate, and copper sulfate. The 7H9 broth was also supplemented with 100 mL/L OADC (oleic acid, bovine albumin, dextrose, and catalase enrichment, from the Becton Dickinson Company) and 0.05% Tween 80. Tween 80 is a detergent added to prevent clumping (Sigma-Aldrich Chemical Co.). Mycobactin J (Allied Monitor) at a final concentration of 2.4 μM was added to the *M. paratuberculosis* strain ATCC 43015 culture as a positive control. When the bacterium was challenged with other siderophores, mycobactin J was not added to the culture media. Siderophores were added to the BACTEC 7H12 B+ bottled liquid media using Becton Dickinson B-D "1 cm^3" sterile syringes to a final concentration of 2.4 μM. To each of these BACTEC bottles, 100 μL of BACTEC 7H12 B+ cultured MAP (with a growth index of 100–300) was inoculated using Becton Dickinson B-D 1 cm^3 sterile syringes. Microbial growth activity in this culture medium is indicated by the release of $^{14}CO_2$ into the atmosphere of the sealed vial following the metabolism of ^{14}C-labeled palmitic acid by the microorganism.

The atmosphere of the sealed BACTEC 12B vial is aspirated from the vial via a sterile needle attached to a robotic arm inside the BACTEC 460 TB Analyzer System. The BACTEC Analyzer operates by initially drawing room air through a dust filter, a flush valve, and an ion chamber transferring all $^{14}CO_2$ into a CO_2 trap, where it is retained. This process cleans the electrometer and leaves it ready to start the next cycle. During the next cycle, a pair of 18G needles are heated. A pump produces a partial vacuum in the ion chamber used to lower the testing needles through the rubber septum of the vial being tested. A vacuum draws culture gas from the vial to the ion chamber. The electrometer measures the very small current that the radioactive $^{14}CO_2$ produces in the ion chamber. Following removal of the radioactive culture gas, fresh 5% CO_2 is introduced into the medium headspace every time a vial is tested, enhancing the growth of mycobacteria. The current measured by the electrometer is amplified and displayed as a numeric reading. The reading is measured on a scale of 0–999 and is an indication of microbial growth activity in the bottle. Usually, a reading of 10 or higher is an indication of definite microbial growth. The growth indices (GI values) listed in Tables 1 and 2 were calculated by dividing the instrument reading obtained for the chelator by that obtained for the mycobactin J control. As is often the circumstance when looking at relative microbiological growth rates over time, the error in making these measurements can be appreciable (up to ±85 reading units). Slow-growing cultures may bias the results as their early growth is more time sensitive, whereas faster-growing cultures may give disproportionately higher values at early sample times. In this regard, one looks for significant differences in growth rates and overall trends.

N^1,N^5($N^{3'}$-**Hydroxyl,**$N^{3'}$-**cinnamoyl-3′aminopropyl)1,5-citric Diamide 8.** TFA (4 mL) was added dropwise to **21** (80 mg, 0.123 mmol) at 0 °C. After the addition was complete, the solution was warmed to room temperature. TLC (15% MeOH/CHCl$_3$) showed that the starting material was consumed after 2 h. The volatiles were removed under high vacuum without heating. The residue was subjected to a LH-20 column (preswelled and eluted with 3% EtOH/toluene) to give **8** (65 mg, 89%). R_f = 0.31 in 15% MeOH/CHCl$_3$; R_f = 0.27 in 15% 2-propanol/ethyl acetate. ^1H NMR (CD$_3$OD): δ 7.64–7.23 (m, 14H, aromatic and olefinic), 3.77 (t, 4H, CH$_2$NO), 3.22 (t, 4H, CH$_2$N), 2.71 (dd, 4H, CH$_2$), 1.86 (m, 4H, CH$_2$); ^{13}C NMR (CD$_3$-OD) δ 177.2, 172.3, 168.1, 143.6, 130.2, 129.8, 128.8, 117.3, 75.2, 47.0, 44.8, 37.7, 27.7. High-resolution mass spectrum: theory for C$_{30}$H$_{37}$N$_4$O$_9$ (M + 1), 597.2561; found M + 1, 597.2534.

N^1,N^5($N^{4'}$-**Hydroxy,**$N^{4'}$-**cinnamoyl-4′aminobutyl)1,5-citric Diamide 9.** TFA (2 mL) was added dropwise to **22** (41

mg, 0.060 mmol) at 0 °C. The mixture was stirred at room temperature. TLC showed the starting material was consumed after 4 h (R_f = 0.56 in 15% MeOH/CHCl₃). The volatiles were removed under high vacuum without heating. The residue was subjected to a Sephadex LH-20 column (preswelled and eluted with 4% EtOH/toluene) to give **9** (32 mg, 84% yield). R_f = 0.38 in 15% MeOH/CHCl₃; R_f = 0.35 in 15% 2-propanol/ethyl acetate. ¹H NMR (CD₃OD): δ 7.64−7.26 (m, 14H, aromatic and olefinic), 3.75 (t, 4H, CH₂NO), 3.20 (t, 4H, CH₂N), 2.70 (q, 4H, CH₂), 1.71 (m, 4H, CH₂), 1.56 (m, 4H, CH₂). ¹³C NMR (CD₃-OD): δ 177.2, 172.0, 168.2, 143.9, 136.3, 131.6, 130.2, 129.0, 117.7, 75.3, 45.2, 40.1, 27.7, 24.8. High-resolution mass spectrum: theory for C₃₂H₄₁N₄O₉ (M + 1), 625.2874; found M+1, 625.2893.

3-(*tert*-Butoxycarbonyl amino)propylamine 12. 1,3-Diaminopropane (**10**) (11.16 g, 150 mmol) was dissolved in 350 mL of a 10% triethylamine (TEA)/MeOH solution. A solution of di-*tert*-butyl dicarbonate (10.9 g, 50 mmol) and MeOH (20 mL) was added to this mixture with vigorous stirring. The solution was refluxed for 2 h and then concentrated under reduced pressure to give an oil. The oil was subjected to flash column chromatography, eluting with 4% NH₄OH/MeOH to give the mono-BOC amine **12** (7.16 g, 82%). R_f = 0.24 in 4% NH₄OH/MeOH. ¹H NMR (CDCl₃): δ 4.95 (br s, 1H, NH), 3.20 (m, 2H, CH₂NC), 2.72 (t, 2H, CH₂N), 1.62 (m, 2H, CH₂), 1.44 (s, 9H, CH₃).

4-(*tert*-Butoxycarbonylamino)butylamine 13. 1,4-Diaminobutane **11** (13.2 g, 150 mmol) was dissolved in 350 mL of 10% TEA/MeOH solution. A solution of di-*tert*-butyl dicarbonate (10.9 g, 50 mmol) and MeOH (20 mL) was added, and the solution was refluxed with vigorous stirring for 2 h. The solution was concentrated and subjected to flash column chromatography, eluting with 2% NH₄OH/MeOH to give the mono-BOC amine **13** (6.96 g, 75%). R_f = 0.27 (2% NH₄OH/MeOH). ¹H NMR (CDCl₃): δ 4.95 (b s, 1H, NH), 3.13 (m, 2H, CH₂NCO), 2.72 (t, 2H, CH₂N), 1.80 (m, 2H, CH₂), 1.60−1.30 (m, 11H, CH₂ and *tert*-butyl). ¹³C NMR (CDCl₃): δ 157.8, 80.8, 43.3, 41.8, 32.3, 29.8, 29.1.

***N*³-Cinnamoyl-*N*³-benzoyloxy-*N*¹-(*tert*-butoxycarbonyl)propane Diamine 14.** A solution of benzoyl peroxide (2.42 g, 10 mmol) and 50 mL CH₂Cl₂ was added dropwise at room temperature to a vigorous stirred mixture of amine **12** (0.87 g, 5 mmol, dissolved in 25 mL CH₂Cl₂) and 75 mL of a carbonate buffer solution (pH 10.5). The starting material was consumed after stirring overnight as shown by TLC (4% NH₄-OH/MeOH). *trans*-Cinnamoyl chloride (0.83 g, 5 mmol) was added dropwise at room temperature. After 30 min, the disappearance of the intermediate (benzoyloxyamine) was monitored by TLC (R_f = 0.43 in 40% ethyl acetate/hexane). After the acylation was complete, the organic layer was separated and the water layer was extracted twice with CH₂-Cl₂. The organic layers were combined, dried over anhydrous Na₂SO₄, filtered, and concentrated. The residue was subjected to flash column chromatography, eluting with 40% ethyl acetate/hexane to give **14** as a white solid (1.16 g, 55%). R_f = 0.51 in 40% ethyl acetate/hexane. ¹H NMR (CDCl₃): δ 8.17 (d, 2H, aromatic), 7.82−7.27 (m, 9H, aromatic and olefinic), 6.66 (d, 1H, olefinic), 5.20 (br s, 1H, NH), 4.00 (t, 2H, CH₂-NO), 3.28 (q, 2H, CH₂N), 1.84 (m, 2H, CH₂), 1.40 (s, 9H, CH₃). ¹³C NMR (CDCl₃): δ 167.7, 164.6, 156.1, 145.0, 134.4, 134.3, 130.1, 129.0, 128.7, 128.2, 126.4, 114.6, 79.2, 46.2, 37.2, 28.3, 27.7.

***N*⁴-Cinnamoyl-*N*⁴-benzoyloxy-*N*¹-(*tert*-butoxycarbonyl)butane Diamine 15.** A solution of benzoyl peroxide (2.96 g, 12.2 mmol) and 50 mL of CH₂Cl₂ was added dropwise at room temperature to a vigorous stirred mixture of amine **13** (1.15 g, 6.1 mmol, dissolved in 50 mL CH₂Cl₂) and 50 mL of a carbonate buffer solution (pH 10.5). The starting material was consumed after stirring overnight as shown by TLC (R_f = 0.27 in 2% NH₄OH/MeOH). *trans*-Cinnamoyl chloride (1.02 g, 6.1 mmol) was added dropwise at room temperature. After 40 min, the disappearance of the intermediate benzoyloxyamine was monitored by TLC (R_f = 0.27 in 33% ethyl acetate/hexane). After the acylation was complete, the organic layer was

separated and the water layer was extracted twice with CH₂-Cl₂. The organic layers were combined, dried over anhydrous Na₂SO₄, filtered, and concentrated. The residue was subjected to flash column chromatography, eluting with 20% ethyl acetate/hexane to give **15** as a white solid (1.39 g, 52%). R_f = 0.41 in 20% ethyl acetate/hexane. ¹H NMR (CDCl₃): δ 8.17 (d, 2H, aromatic), 7.81−7.28 (m, 9H, aromatic and olefinic), 6.68 (d, 1H, olefinic), 4.60 (br s, 1H, NH), 3.98 (t, 2H, CH₂-NO), 3.18 (m, 2H, CH₂N), 1.70 (m, 4H, CH₂), 1.40 (s, 9H, CH₃). ¹³C NMR (CDCl₃): δ 166.7, 164.4, 156.1, 145.6, 134.8, 134.7, 130.2, 129.0, 128.8, 128.0, 126.8, 114.6, 79.0, 48.6, 40.2, 28.7, 27.6, 24.2.

***N*³-Hydroxyl-*N*³-cinnamoyl-*N*¹-BOC-propane Diamine 16.** A solution of 10% NH₄OH/MeOH (25 mL) was added dropwise to **14** (0.9483 g, 2.23 mmol) in a pretreated iron-free round-bottom flask at 0 °C. The mixture was stirred overnight under N₂ atmosphere. The disappearance of the starting material was monitored by TLC (R_f = 0.61, 50% ethyl acetate/hexane). The mixture was concentrated, and the product was recrystallized using ethyl acetate and hexane (1:5 volume ratio) to give a white solid **16** (0.60 g, 81%). R_f = 0.23 (50% ethyl acetate/hexane); mp 92.0−93.0 °C. ¹H NMR (CDCl₃): δ 9.35 (br s, 1 H, OH), 7.10−7.70 (m, 7H, aromatic and olefinic), 5.21 (br s, 1H, NH), 3.81 (t, 2 H, CH₂NO), 3.19 (q, 2 H, CH₂N), 1.86 (m, 2H, CH₂), 1.40 (s, 9 H, CH₃). ¹³C NMR (CDCl₃): δ 167.0, 157.1, 142.7, 135.2, 129.8, 128.8, 128.1, 116.4, 80.0, 46.7, 37.3, 28.2, 27.3.

***N*⁴-Hydroxyl-*N*⁴-cinnamoyl-*N*¹-BOC-butane Diamine 17.** In a 50 mL pretreated iron-free round-bottom flask, 10% NH₄OH/CH₃OH (20 mL) was added dropwise to **15** (0.85 g, 1.94 mmol) at 0 °C under an Ar atmosphere. The disappearance of the starting material was monitored by TLC (R_f = 0.79, 70% ethyl acetate/hexane). The mixture was concentrated, and the product was recrystallized with methanol and hexane (1:4 volume ratio) to give **17** as a white solid (0.61 g, 94%). R_f = 0.56 (70% ethyl acetate/hexane); mp 140.0−142.0 °C. ¹H NMR (CD₃OD): δ 7.65−7.23 (m, 7H, aromatic and olefinic), 3.72 (t, 2H, CH₂NO), 3.10 (t, 2H, CH₂N), 1.68 (m, 2H, CH₂), 1.4 (m, 11 H, CH₂ and *tert*-butyl). ¹³C NMR (CD₃OD): δ 168.2, 158.3, 143.8, 136.3, 130.3, 129.8, 128.5, 117.7, 80.0, 48.5, 40.4, 28.6, 28.2, 25.1.

***N*³-Hydroxyl-*N*³-cinnamoyl-propane Diamine Trifluoroacetic Acid Salt 18.** Trifluoroacetic acid (TFA, 10 mL) was added dropwise over 2 min to **16** (44 mg, 0.137 mmol) at 0 °C. The ice bath was removed, and the solution was stirred for 30 min. TLC (40% ethyl acetate/hexane) showed that the reaction was complete. The volatiles were removed under reduced pressure to give the desired salt **18** as a crude oil, which was consumed in the next step. ¹H NMR (CD₃OD): δ 7.89−7.24 (m, 7H, aromatic and olefinic), 3.88 (t, 2H, CH₂NO), 2.98 (t, 2H, CH₂N), 2.07 (m, 2H, CH₂). ¹³C NMR (CD₃OD): δ 169.0, 144.2, 136.2, 131.7, 129.8, 128.6, 116.7, 46.2, 38.2, 26.1.

***N*⁴-Hydroxyl-*N*⁴-cinnamoyl-*N*¹-BOC-butane Diamine Trifluoroacetic Acid Salt 19.** Using a similar process, TFA (15 mL) was combined with hydroxamic acid **17** (0.49 g, 1.46 mmol) at 0 °C and stirred for 2 h. TLC (60% ethyl acetate/hexane) showed that the reaction was complete. The volatiles were removed under reduced pressure to give the desired salt **19** as a crude oil, which was consumed in the next step. ¹H NMR (CD₃OD): δ 7.66−7.28 (m, 7H, aromatic and olefinic), 3.81 (t, 2H, CH₂NO), 2.97 (t, 2H, CH₂N), 1.79 (m, 4H, CH₂). ¹³C NMR (CD₃OD): δ 168.3, 144.0, 136.2, 131.6, 130.0, 129.1, 117.2, 48.3, 40.1, 25.7, 24.4.

2-*tert*-Butyl-1,3-di-*N*-(hydroxyl) Succinimidyl Citrate (NHS Ester) 20. 3-*tert*-Butyl citrate **25** (4.60 g, 18.5 mmol) and *N*-hydroxy succinimide (4.27 g, 37 mmol) were dissolved in 100 mL of dry THF. A *N,N*-diisopropylcarbodiimide (DIC) solution (3.34 g, 29 mmol dissolved in 100 mL dry THF) was added dropwise to the solution at room temperature. The mixture was stirred for 2 days. A white precipitate formed. The ¹H NMR spectrum of the mixture showed that the reaction was complete (i.e., the multiplet signal at 2.80 ppm disappeared). The mixture was filtered, and the white precipitate was kept. ¹H NMR showed the precipitate contained the

product and diisopropyl urea (doublet at 1.1 ppm). Hot $CHCl_3$ was added to the crude solid, and part of the precipitate dissolved. The mixture was filtered, and the solid was collected and air-dried overnight to give the NHS ester **20** as a white solid (1.64 g, 20%). ^1H NMR (DMSO-d_6): δ 3.33 (d, 2H, CH_2), 3.21 (d, 2H, CH_2), 2.80 (s, 8H, CH_2), 1.40 (s, 9H, CH_3). ^{13}C NMR (DMSO-d_6): δ 170.0, 165.0, 81.0, 72.1, 38.9, 27.1, 24.7.

$N^4,N^5(N^{3'}$-Hydroxy,$N^{3'}$-cinnamoyl-3'-aminopropyl)-3-tert-butoxycarbonyl-1,5-citric Diamide 21. In a pretreated iron-free round-bottom flask, TEA (0.7 g, 6.94 mmol) was added to a mixture of 2-tert-butyl-1,3-di-N-succinimidyl citrate (NHS ester **20**) (0.1317 g, 0.298 mmol) and TFA amine salt **18** (0.2106 g, 0.63 mmol) dissolved in 50 mL of dry dioxane at 0 °C. The solution was allowed to warm to room temperature and stirred overnight. The solvent was removed under reduced pressure, and the residue was dissolved in $CHCl_3$ (20 mL) and washed with 0.5 N HCl (20 mL). The aqueous layer was extracted twice with $CHCl_3$. The organic layers were combined and concentrated. The residue was subjected to a Sephadex LH-20 column (preswelled and eluted with 4% EtOH/toluene) to give **21** as a solid (0.175 g, 90%). R_f = 0.26 in 10% MeOH/$CHCl_3$. ^1H NMR ($CDCl_3$): δ 9.70 (br s, 1H, OH), 7.63−7.24 (m, 14H, aromatic and olefinic), 3.78 (t, 4H, CH_2NO), 3.24 (q, 4H, CH_2N), 2.64 (dd, 4H, CH_2), 1.84 (m, 4H, CH_2), 1.41 (s, 9H, CH_3). ^{13}C NMR ($CDCl_3$): δ 172.9, 170.3, 167.1, 142.9, 134.9, 129.9, 128.8, 127.9, 116.5, 83.2, 73.9, 46.5, 44.2, 36.6, 27.8, 26.6. High-resolution mass spectrum: theory for $C_{34}H_{45}N_4O_9$ (M + 1), 653.3187; found M + 1, 653.3117.

$N^4,N^5(N^{4'}$-Hydroxy,$N^{4'}$-cinnamoyl-4'aminobutyl)-3-tert-butoxycarbonyl-1,5-citric Diamide 22. TEA (5.11 g, 50 mmol) was added dropwise to a mixture of NHS ester **20** (0.74 g, 1.67 mmol) and **19** (1.17 g, 3.37 mmol) in 60 mL of dry dioxane at 0 °C. The solution was allowed to warm to room temperature and stirred overnight. The volatiles were removed under reduced pressure. The residue was subjected to a Sephadex LH-20 column (preswelled and eluted with 5% EtOH/toluene) to give **22** as a solid (0.97 g, 85%). R_f = 0.30 in 10% MeOH/$CHCl_3$. ^1H NMR ($CDCl_3$): δ 9.80 (br s, 1H, OH), 7.61−7.21 (m, 14H, aromatic and olefinic), 3.72 (t, 4H, CH_2-NO), 3.17 (q, 4H, CH_2N), 2.68 (dd, 4H, CH_2), 1.67−1.35 (m, 14H, tert-butyl and 2 CH_2). ^{13}C NMR ($CDCl_3$): δ 172.1, 169.3, 166.1, 141.9, 133.9, 128.9, 127.9, 127.6, 115.7, 82.1, 73.6, 47.2, 42.6, 38.0, 26.4, 25.7, 22.6. High-resolution mass spectrum: theory for $C_{36}H_{49}N_4O_9$ (M + 1), 681.3500; found M + 1, 681.3474.

1,5-Dimethyl Citrate 23. Concentrated H_2SO_4 (1 mL) was added dropwise to a solution of citric acid (50 g, 0.26 mole) and MeOH (250 mL) at room temperature. The mixture was refluxed for 1 h. Lime water (75 g $CaCO_3$ suspended in 1 L water) was used to neutralize the solution to pH 7.0. A white precipitate formed, which was filtered off and discarded. The filtrate was concentrated down under vacuum to give a white residue. Water (100 mL) was added to the residue. The mixture was sonicated and filtered. The filtered solid was discarded, and the filtrate was kept. Concentrated HCl was added to bring the filtrate to pH 0. A white precipitate formed and was filtered and kept. The precipitate was dissolved in 8% (w/w) $NaHCO_3$ solution (25 mL). The solution was washed three times using $CHCl_3$. Then, concentrated HCl was added again to bring the solution to pH 0. Again, a white precipitate was formed. This material was filtered and dried to give 1,5-dimethyl citrate **23** as a white solid (20.0 g, 35%). ^1H NMR (CD$_3$OD): δ 3.67 (s, 6H, CH_3), 2.87 (dd, 4H, CH_2).

tert-Butyl-1,5-dimethyl Citrate 24. Concentrated perchloric acid (2.7 mL, 0.03 mole) was added to a solution containing 1,5-dimethyl citrate **23** (20 g, 0.09 mole) and tert-butyl acetate (120 mL, 0.89 mole). The solution was stirred at room temperature for 3 days under N_2. A saturated aqueous $NaHCO_3$ solution was used to bring the solution to pH 6. The organic layer was separated. The aqueous layer was extracted three times using CH_2Cl_2. The organic layers were combined and concentrated down to give a yellow residue. The residue was dissolved in hot hexane (400 mL). The solution was allowed to cool slowly to room temperature and then placed

in a refrigerator until a white precipitate formed (possibly a trimethyl citrate impurity). The precipitate was filtered and discarded. The filtrate was concentrated to give 3-tert-butyl-1,5-dimethyl citrate **24** as a light yellow oil (18.7 g, 75%). ^1H NMR ($CDCl_3$): δ 3.70 (s, 6H, CH_3), 2.84 (m, 4H, CH_2), 1.52 (s, 9H, CH_3).

3-tert-Butyl Citrate 25. 3-tert-Butyl-1,5-dimethyl citrate **24** (16 g, 58 mmol) was dissolved in MeOH (58 mL). A chilled 2 M NaOH aqueous solution (58 mL) was added to the solution at 0 °C. The mixture was warmed to room temperature and stirred for 3 h. Two layers formed. The organic layer was discarded. The aqueous layer was acidified to pH 2 using 2 N HCl. The aqueous layer was extracted with ethyl acetate three times. The ethyl acetate layers were combined and concentrated down to give 3-tert-butyl citrate **25** as a white solid 7.89 g (55%). ^1H NMR (CD$_3$OD): δ 2.80 (dd, 4H, CH_2), 1.50 (s, 9H, CH_3).

References

(1) World Health Organization. *Global Tuberculosis Control*; WHO Report 2001; World Health Organization: Geneva, Switzerland; WHO/CDS/TB/2001.287

(2) World Health Organization Tuberculosis Fact Sheet, No. 104, 2000; see http://www.who.int/inf-fs/en/fact104.html.

(3) (a) Miller, M. J. Synthesis and Therapeutic Potential of Hydroxamic Acid Based Siderophores and Analogues. *Chem. Rev.* **1989**, *89*, 1563−1579. (b) Haeym, B., Honoré, N.; Truffot-Pernot, C.; Banerjee, A.; Schurra, C.; Jacobs, W. R., Jr.; van Embden, J. D. A.; Grosset, J. H.; Cole, S. T. Implications of Multidrug Resistance for the future of Short Course Chemotherapy of Tuberculosis: A Molecular Study. *Lancet* **1994**, *344*, 293−298.

(4) Salyers, A. A.; Whitt, D. D. *Bacterial Pathogenesis: A Molecular Approach*, 1st ed.; ASM Press: Washington, DC, 1994.

(5) (a) Rouhi, A. M. Tuberculosis: A Tough Adversary. *Chem. Eng. News* **1999**, *May 17*, 52−69. (b) Xu, Y.; Miller, M. J. Total Syntheses of Mycobactin Analogues as Potent Antimycobacterial Agents Using a Minimal Protecting Group Strategy. *J. Org. Chem.* **1998**, *63*, 4314−4322.

(6) (a) Connell, N. D.; Nikaido, H. Membrane Permeability and Transport in Mycobacterium Tuberculosis. In *Tuberculosis: Pathogenesis, Protection, and Control*; Bloom, B. R., Ed.; ASM Press: Washington, DC, 1994; p 333. (b) Besra, G. S.; Chatterjee, D. Lipid and Carbohydrates of Mycobacterium Tuberculosis. In *Tuberculosis: Pathogenesis, Protection, and Control*; Bloom, B. R., Ed.; ASM Press: Washington, DC, 1994; p 285.

(7) Malouin, F.; Miller, M. J. Microbial Iron Chelators as Drug Delivery Agents: The Rational Design and Synthesis of Siderophore-Drug Conjugates. *Acc. Chem. Res.* **1993**, *26*, 241−249.

(8) Lin, Y.; Helquist, P.; Miller, M. J. Synthesis and Biology Evaluation of a Siderophore-Virginiamycin Conjugate. *Synthesis* **1999**, *No. SI*, 1510−1514.

(9) (a) Bergeron, R. J.; Brittenham, G. M. *The Development of Iron Chelators for Clinical Use*; CRC Press: Boca Raton, FL, 1994; pp 279−284. (b) Bergeron, R. J.; Brittenham, G. M. *The Development of Iron Chelators for Clinical Use*; CRC Press: Boca Raton, FL, 1994; p 258.

(10) Roosenberg, J. M., II; Lin, Y.-M.; Lu, Y.; Miller, M. J. Studies and Syntheses of Siderophores, Microbial Iron Chelators, and Analogues as Potential Drug Delivery Agents. *Curr. Med. Chem.* **2000**, *7*, 159−197 and references therein.

(11) (a) Barclay, R.; Ratledge, C. Iron binding compounds of *M. avium, M. intracellularae, M. scrofulaceum*, and mycobactin-dependent *M. paratuberculosis* and *M. avium. J. Bacteriol.* **1983**, *153*, 1138−1146. (b) Chamberlin, W.; Graham, D. Y.; Hulten, K.; El-Zimaity, H. M. T.; Schwartz, M. R.; Naser, S.; Shafran, I.; El-Zaatari, F. A. K. *Mycobacterium avium* subsp. *Paratuberculosis* as one cause of Crohn's disease. *Aliment Pharmacol. Ther.* **2001**, *15*, 337−346. (c) Chiodini, R. J.; Van Kruiningen, H. J.; Merkal, R. S. Ruminant paratuberculosis (Johne's Disease): The current status and future prospects. *Cornell Vet.* **1984**, *74*, 218−262.

(12) Guo, H. Synthesis of New Citrate-Based Siderophores As Potential Drug Delivery Agents for Mycobacterium Paratuberculosis and the Reactions of *N*-(Benzoyloxy)hexylamine with Ketones and Aldehydes. Masters Thesis, Department of Chemistry, University of Central Florida, 2000.

(13) (a) McCullough, W. G.; Merkal, R. S. Structure of Mycobactin J. *Curr. Microbiol.* **1982**, *7*, 337−341. (b) Mathews, P. R.; McDiarimid, J. A.; Collins, P.; Brown, A. The Dependence of some strains of *M. avium* on mycobactin for initial and subsequent growth. *J. Med. Microbiol.* **1979**, *11*, 53−57. (c) Lambrecht, R. S.; Collins, M. T. Mycobacterium paratuberculosis. Factors that influence mycobactin dependence. *Diagn. Microbiol. Infect. Dis.* **1992**, *15* (3), 239−246.

(14) Phanstiel, O., IV; Wang, Q. Total Synthesis of Acinetoferrin. *J. Org. Chem.* **1998**, *63*, 1491−1495.

(15) Bergeron, R. J.; McManis, J. S.; Phanstiel, O., IV; Vinson, J. R. T. Total Synthesis of DFO. *J. Org. Chem.* **1995**, *60*, 109−114.

(16) Milewska, M. J.; Chimiak, A. I.; Glowacki, Z. Synthesis of Schizokinen, Homoschizokinen, Its Imide and the Detection of Imide with ¹³C NMR Spectroscopy. *J. Prakt. Chem.* **1987**, *329* (3), 447−456.

(17) (a) Maurer, P. J.; Miller, M. J. Total Synthesis of a Mycobactin: Mycobactin S2. *J. Am. Chem. Soc.* **1983**, *105*, 240−245. (b) Hu, J.; Miller, M. J. Total Synthesis of a Mycobactin S, a Siderophore and Growth Promoter of Mycobacterium Smegmatis, and Determination of its Growth Inhibitory Activity against *Mycobacterium tuberculosis*. *J. Am. Chem. Soc.* **1997**, *119*, 3462−3468. (c) Hu, J. Total Synthesis of Mycobactins, Siderophore-Drug Conjugates and Biological Studies. Ph.D. Dissertation, Department of Chemistry and Biochemistry, University of Notre Dame, 1996.

(18) Bergeron, R. J.; Phanstiel, O., IV. The Total Synthesis of Nannochelin: A Novel Cinnamoyl Hydroxamate Containing Siderophore. *J. Org. Chem.* **1992**, *57*, 7140−7143.

(19) Milewska, M. J.; Chimiak, A. An Alternative Synthesis of N^5-Acetyl-N^5-hydroxy-L-ornithine from L-Ornithine. *Synthesis* **1990**, 233−234.

(20) Wang, Q. X,; King, J.; Phanstiel, O., IV. An Improved Synthesis of *O*-Benzoyl Protected Hydroxamates. *J. Org. Chem.* **1997**, *62*, 8104−8108.

(21) Phanstiel, O., IV; Wang, Q. X.; Powell, D. H.; Ospina, M. P.; Leeson, B. A. Synthesis of Secondary Amines via *N*-(Benzoyloxy)-amines and Organoboranes. *J. Org. Chem.* **1999**, *64*, 803−806.

(22) Badescu, V. Synthesis and Thermal Study of a Series of *N*-Benzoyloxyamines and the Scope and Limitations of an Amine Oxidation Process. Masters Thesis, Department of Chemistry, University of Central Florida, 2000.

(23) Lee, B. H.; Miller, M. J. Microbial Iron Chelators: Total Synthesis of Aerobactin and Its Constituent Amino Acid, N^6-Acetyl-N^6-hydroxylysine. *J. Am. Chem. Soc.* **1982**, *104*, 3096−3101.

(24) Benoiton, N. L.; Chen, F. M. F. Not the Alkoxycarbonylamino acid *O*-Acylisourea. *Chem. Commun.* **1981**, 543−545.

(25) Naser, S. A.; Gillespie, R.; Naser, N. A.; El-Zaatari, F. A. K. Effect of IS900 gene of *Mycobacterium paratuberculosis* on *Mycobacterium smegmatis*. *Curr. Microbiol.* **1998**, *37* (6), 373−379.

(26) Johnsson, K.; King, D. S.; Schultz, P. G. Studies on the mechanism of Action of Isoniazid and Ethionamide in the Chemotherapy of Tuberculosis. *J. Am. Chem. Soc.* **1995**, *117*, 5009−5010.